Nuclear Inst. and Methods in Physics Research, A 1040 (2022) 167087

Contents lists available at ScienceDirect

Nuclear Inst. and Methods in Physics Research, A

journal homepage: www.elsevier.com/locate/nima

Synthesis of solid mercury targets for nuclear astrophysics experiments

Khushi Bhatt *, Shivi Saxena, Michael Famiano, Ramakrishna Guda, Asghar Kayani, Zbigniew Chajecki

Western Michigan University, 1903 W Michigan Ave, Kalamazoo, 49008, MI, USA

ARTICLE INFO

Keywords:
Targets
Nuclear physics

ABSTRACT

This paper describes several simple and cost-effective ways of making homogeneously thin solid mercury targets useful for nuclear astrophysics experiments at standard ambient temperature and pressure and in vacuum. The methods described here make use of mercury compounds such as mercury(II) acetate, mercury(II) oxide (yellow), mercury(II) chloride, mercury (II) nitrate monohydrate, and mercury(II) sulfide (red). Various methods like drop-casting, wet chemistry, electro-chemical deposition, amalgamation, and pelletization are described. Advantages and disadvantages of each method are described.

1. Introduction

The common characteristics desired in typical targets include homogeneous concentration, uniform thickness, and strength to survive beam irradiation. Production methods depend upon factors like the starting chemical, physical form (powder, paste etc.), desired thickness, whether it is self supporting or on a substrate etc. Targets used in the field of nuclear astrophysics for measuring cross-sections at low energy may have an areal density of ~1 μg/cm^2 to 10–20 mg/cm^2 [1] or more depending on the application.

Synthesis of a solid mercury target is difficult owing to the toxicity of Hg and many of its compounds as well as the fact that natural Hg is a liquid at room temperature. The method used for target preparation should produce a target of uniform desired thickness while maximizing the purity of Hg in the target.

As elemental mercury occurs in the liquid state, one possibility is to use mercury compounds for the synthesis of a solid target. Mercury compounds like mercury(II) acetate ($Hg(O_2CCH_3)_2$), yellow mercury(II) oxide (HgO), mercury(II) chloride ($HgCl_2$), mercury(II) nitrate monohydrate ($Hg(NO_3)_2{\cdot}H_2O$), and red mercury(II) sulfide (HgS) are studied here with various production methods. Prior production methods using Hg compounds make use of high temperature processing [2, 3]. Targets synthesized at lower temperatures [4] resulted in a very thick target and would not be useful for low energy nuclear-cross section measurements.

Here, we describe several methods used to produce cost-effective Hg targets at standard ambient temperature and pressure using Hg compounds. The thickness of the target is nominally 10 mg/cm^2 (~ 8 - 30 μm depending upon the density of the compound), useful for conducting low energy experiments at astrophysically relevant energies.

2. Methods of synthesis

2.1. Pelletization

The pelletization method — also known as the powder pressing or tablet pressing method has been studied to create a self-supporting target. Powder is placed into a cavity between two flat surfaces of the die assembly (shown in Fig. 1) of a Fourier Transform Infrared (FTIR) pellet press. The powder of interest is ground using a mortar and pestle to reduce individual particle size.

The die assembly is compressed using a manual hydraulic press (shown in Fig. 2). Air is pumped out simultaneously. For targets produced here, the diameter of the cavity was 15 mm. Mercury compounds $Hg(O_2CCH_3)_2$, HgO, $HgCl_2$, $Hg(NO_3)_2$, and HgS were tested with this method. The mesh size information of HgS provided by supplier (Millipore Sigma) is remainder through 300 mesh: 1.5% maximum. The powder sizes or mesh numbers for other compounds are not available as the manufacturers have not tested this parameter. $Hg(OAc)_2$ and HgO were also tried in combination with potassium bromide (KBr). Between 10 mg and 50 mg of individual compounds were tested. In each test, a proper pellet was not obtained using any of the compounds considered. It was determined that the hygroscopic nature of $Hg(O_2CCH_3)_2$ resulted in a brittle pellet adhering to the die assembly. The pellet broke upon separation from the die. Further it was also found that thin target could not be reliably produced as the small volume of compound could not be uniformly distributed between the dies consistently. Attempts were made to make a pellet by placing the powder between two weighing paper pieces to avoid the attachment of the pellet with the die, but these were not successful.

* Corresponding author.
E-mail address: khushi.bhatt@wmich.edu (K. Bhatt).

https://doi.org/10.1016/j.nima.2022.167087
Received 12 February 2022; Received in revised form 2 June 2022; Accepted 26 June 2022
Available online 3 July 2022
0168-9002/

Fig. 1. The die assembly used for pelletization using a hydraulic press. The black bottom acts as an assembly holder and can be connected to a vacuum pump while pressing. The two circular discs are the dies between which the powder is placed and the cylindrical rod helps in applying pressure uniformly during pressing.

Fig. 2. The hydraulic press used for pelletization along with the die assembly in place. A detachable vacuum pump was attached for simultaneous pumping out of air for more compact pellet making.

Uniform tablets of thickness 26.67 mg/cm^2 were obtained with HgO and HgS by using 40 mg of powder. This would place a lower limit on applications requiring thin targets [1] using this technique. These might be useful in thick target applications.

2.2. Wet-chemistry

It was found that finer particles result in better uniformity and strength. In order to obtain the finest possible particles, wet chemistry methods were incorporated where the compound required for deposition was produced *in situ* through chemical reactions in the solution. The sizes of the particles obtained through wet-chemistry methods are not measured. The rate of production of particles and the rate of deposition was controlled through the concentration of the solution and the duration for which the substrate was left for deposition.

This method is based on the previous work of Perakh and Ginsburg [5] using $HgCl_2$ and sodium sulfide nonahydrate ($Na_2S{\cdot}9H_2O$).

By dissolving a compound, HgS was produced as a precipitate using the following reaction:

$$HgCl_2 + Na_2S \Longrightarrow HgS \downarrow +2NaCl \quad (1)$$

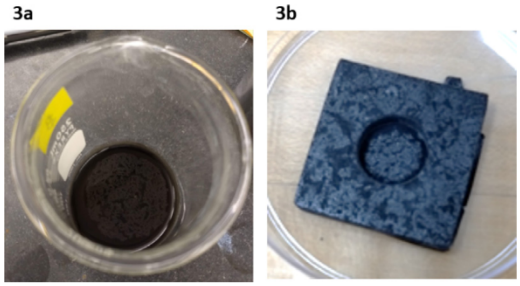

Fig. 3. Target synthesis by wet chemistry: deposition of HgS produced in situ.

Two solutions were explored with this method. One solution, Solution 1 (S1) was made by dissolving 4.8 mg of $HgCl_2$ in 20 ml distilled water through sonication. After the initial solution was prepared, 12.9 mg of $Na_2S{\cdot}9H_2O$ was added to the solution and mixed well using sonication to obtain a homogeneous mixture. A second solution, Solution 2 (S2), was made by dissolving 48.0 mg of $HgCl_2$ in 20 ml distilled water through sonication. After dissolving, 129.0 mg of $Na_2S{\cdot}9H_2O$ was added to the solution and mixed well using sonication to obtain a homogeneous mixture. Aluminized mylar (Al-mylar) and silicon sheets were used as substrates. The substrate was immersed in these solutions to allow the HgS to precipitate onto it.

After leaving the substrate in the solution, the solution was slowly and carefully drawn out using a micro-pipette. Durations of 10, 12, 18, 22, 48 and 72 h were tried. After removing the maximum amount of solution possible, the rest was allowed to dry until a solid deposition was obtained.

To sparge the solution, high pressure (~ 200–400 kPa) nitrogen gas was injected into a paraffin-covered beaker containing the solution and the substrate. The nitrogen acted as an inert gas to displace oxygen.

The aluminum of Al-mylar dissolved in the solution within 5 min. The reaction of Hg with the aluminum on the mylar rendered the substrate uneven, leading to non-uniform deposition. The lower surface of the substrate of the target made with S2 was undamaged, however it was hypothesized that $HgCl_2$ reacted with aluminum in the absence of $Na_2S{\cdot}9H_2O$, but in its presence Hg reacted with S making HgS.

Targets made with S1 resulted in no deposition whereas S2 resulted in a uniform deposition. In the case of S2, it was found that some HgS particles had already begun to precipitate prior to immersion of the substrate. Several precipitate particles were floating on the surface of the solution. As the solution was removed, these particles descended down and settled on the upper layer of deposition, resulting in significant non-uniformity.

Instead of adding $Na_2S{\cdot}9H_2O$ to the $HgCl_2$ solution, two separate solutions were made. A solution was made by dissolving 48.0 mg of $HgCl_2$ in 10 ml distilled water through sonication; and another solution was made by dissolving 129 mg of $Na_2S{\cdot}9H_2O$ in 10 ml distilled water through sonication. The substrate was immersed in the $Na_2S{\cdot}9H_2O$ solution and $HgCl_2$ solution was slowly added. This method slows the rate of HgS production thus producing finer particles and more uniform deposition. However, several precipitate HgS particles that float to the surface of the solution descended on the upper layer of deposition and made the target non-uniform. Fig. 3 (a) shows the black suspension at the end of deposition period and (b) shows the obtained target after drying.

Another reaction was explored to produce HgO precipitation onto a substrate:

$$Hg(NO_3)_2 + 2KOH \Longrightarrow HgO \downarrow +2KNO_3 + H_2O \quad (2)$$

This was made by dissolving 0.5 g of $Hg(NO_3)_2$ in 50 ml distilled water through sonication. After this, 90 mg of KOH was added to the solution and stirred well. As the *in situ* production of HgO begins immediately after the addition of KOH, the substrate was quickly inserted

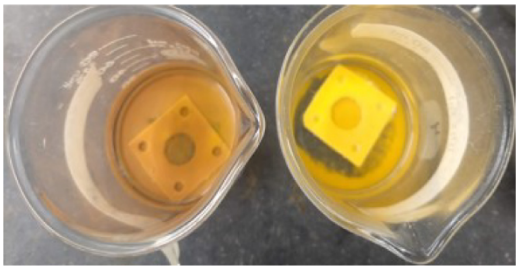

Fig. 4. Target synthesis by wet chemistry: deposition of HgO produced in situ.

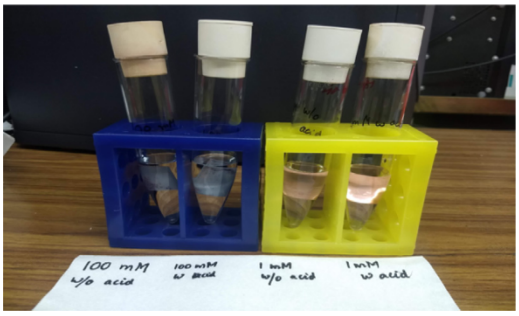

Fig. 5. Amalgamation obtained on the surface of a copper sheet with 1 mM and 10 mM solution of $Hg(NO_3)_2$ with and without acidification of solution with 70% concentrated HNO_3, at the end of 1 h.

after the addition of KOH. Nearly uniform deposition was obtained. As this method had no issues of tiny HgO particles floating to the surface of the solution, this deposition was preferable to the HgS deposition through wet chemistry. Fig. 4 shows the yellow suspension deposited at the end of deposition period.

2.3. Amalgamation

Amalgamation was attempted using copper sheets in $Hg(NO_3)_2$ solutions of concentrations 1 mM, 10 mM and 100 mM. The copper sheet was cleaned by first sonicating it in 99% glacial acetic acid, followed by placing it into a solution of baking soda and water, and rinsing in distilled water. The sheet was then wiped dry.

As the amalgamation occurs in an uncontrolled manner naturally the resulting amalgam was not uniformly thick. A 1 mM solution gave no amalgamation, whereas a 100 mM solution resulted in an uneven silver-colored layer. To check the dependence of target uniformity on solution pH, a few drops of acid were added, but no difference was observed. Fig. 5 shows the amalgamation obtained on copper sheet using 1 mM and 100 mM solution with and without addition of acid drops.

An attempt of amalgamation was made on aluminum foil with 10 mM $Hg(NO_3)_2$ solution, the foil was destroyed by the solution as shown in Fig. 6.

2.4. Electro-chemical deposition

A thin layer of a desired metal's deposition can be obtained on a conductive substrate of interest through electro-chemical deposition. The deposition of metal is obtained via electrolysis using a solution containing the desired metal ions. A potential is then applied to an electrode in the solution. The value of potential at which a sharp increase in reduction current (the current generated by the production of negatively charged chemical species at an electrode) is obtained is called the *onset potential* and is an indicator that deposition is occurring. During electro-deposition, various kinetic and thermodynamic barriers

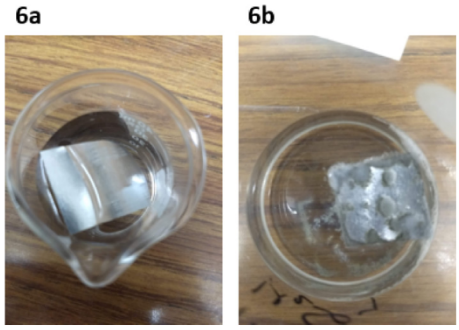

Fig. 6. Images taken during the amalgamation with aluminum. (a) shows when the aluminum foil was being dipped in to the 10 mM $Hg(NO_3)_2$ solution, and (b) shows the aluminum foil after about 20 min.

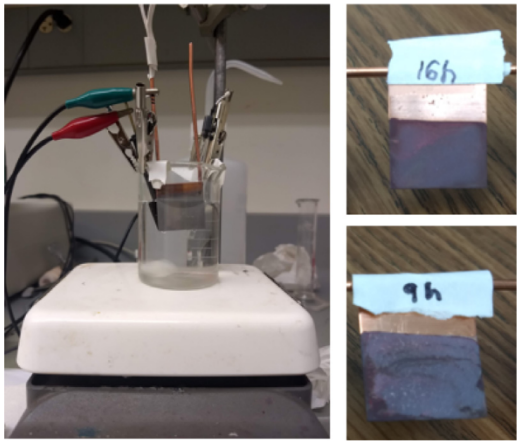

Fig. 7. Figure (left) shows the setup used for electro-chemical deposition of Hg on copper sheet, deposition of Hg on copper sheet after 16 h (top), and after 9 h (bottom).

act against the reduction of mercuric ions, hence operating at the onset potential helps in overcoming the barriers. An electro-chemical workstation (model CHI440 A) from CH Instruments was used here (shown in Fig. 7). A copper sheet was used as a substrate and a solution of $Hg(NO_3)_2{\cdot}H_2O$ powder in distilled water was used as the electrolyte solution.

The substrate acts as a working electrode, Ag/AgCl was used as a reference electrode, and a platinum disc acts as counter electrode. Concentrations of 1 mM, 10 mM and 100 mM were used for studying electro-chemical deposition. The $Hg(NO_3)_2$ solution was obtained by dissolving 68.54 mg, 685.4 mg and 6854 mg of $Hg(NO_3)_2{\cdot}H_2O$ powder respectively in 200 ml distilled water.

Linear Sweep Voltammetry (LSV) was performed in a voltage range of 0 to −1 V to determine the onset potentials (as the Mercury (II) ion has positive charge) [6] as shown in Fig. 8. This was followed by a chrono-amperometry technique for the deposition, where the initial voltage applied was equal to the onset potential values for each solution. The desired time for electrochemical deposition was then set. The onset potential for 1 mM, 10 mM and 100 mM solutions were −0.74, −0.76 and −0.78 V respectively.

The electro-chemical deposition gives a solid deposition, because mercury forms an amalgam with the copper. Electro-chemical deposition was attempted for durations of 10 min, 30 min, 60 min, 120 min, 4 h, 9 h, 16 h and 25 h. As the uniformity of deposition was dependent on pH of the solution, HNO_3 acid was used to decrease the pH, leading to more compact and homogeneous deposition. If the electro-chemical deposition was carried for longer duration, then elemental mercury droplets were seen on the surface of mercury-copper amalgam, as no copper was exposed on the anode.

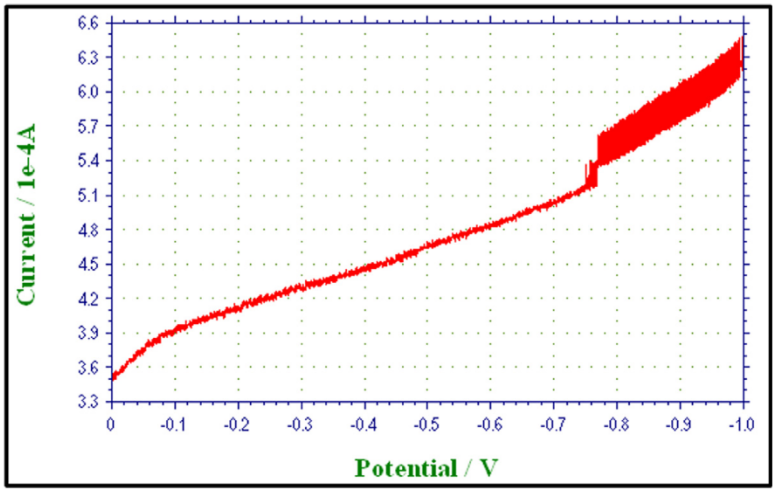

Fig. 8. LSV plot of Copper sheet dipped in 10 mM solution of $Hg(NO_3)_2$, with onset potential at −0.76 V.

The deposition rate was non-constant due to the fact that as the electrolysis takes place, the metal ions are taken from the solution near the surface of the copper resulting in a decreasing concentration of metal ions available near surface. To counteract this, a magnetic stirrer was placed in the beaker to maintain a uniform concentration through the solution.

Adding the magnetic stirrer improved the level of uniformity. However, the deposition was not uniform over the surface area. The process of amalgamation begins on the surface of copper sheet immediately. This is because during the time it takes to obtain the onset potential through LSV, an uncontrolled amalgamation already takes place on the surface making the surface uneven.

Copper substrates suffer from the additional drawback of having very large proton capture cross-sections. For activation-type experiments based on counting decay photons, this would result in a large number of emitted photons, which would potentially affect the live time of a counting system.

2.5. Drop-casting

In this method a drop of liquid solution or suspension is cast onto a substrate of interest and the solution is allowed to slowly evaporate to produce a thin film deposited on the surface. The evaporation area is covered using a loose petri dish lid. Several compounds were tested with this method, and HgS was found to produce satisfactory uniform targets of varying thickness. The substrate was made by cutting a circular cavity in G10 material and aluminum foil of 6 μm or 3 μm or Al-mylar of 2 μm was glued to its surface on one side (We note that the substrate may create a background in certain experiments). The targets obtained were primarily observed under a microscope to inspect the uniformity of the deposition.

Several other compounds are described below:

$Hg(O_2CCH_3)_2$: $Hg(O_2CCH_3)_2$ solutions of concentration 1 mg/ml and 5 mg/ml in water as well as in methanol were tried with drop sizes of 40 μl and 90 μl, resulting in non-uniform targets. The non-uniformity of the target, determined by observing the target under a microscope, was found to be higher than 0.8%. The evaporation rate of methanol was too fast whereas that of distilled water was too slow, as shown in Table 1. If the rate of evaporation of the solvent is fast, particles will not have enough time to redistribute in the solution and bind to the surface evenly. The hygroscopic nature of mercury acetate also hindered obtaining a uniform target.

HgO: In this method a homogeneous suspension of HgO was used for drop casting. Various solvents and mixtures of solvents were considered for making the solution. HgO is insoluble in alcohol, ether, acetone and ammonia, and it is partially soluble in water with solubility of 53 μg/ml at 25 °C and 395 μg/ml at 100 °C [7].

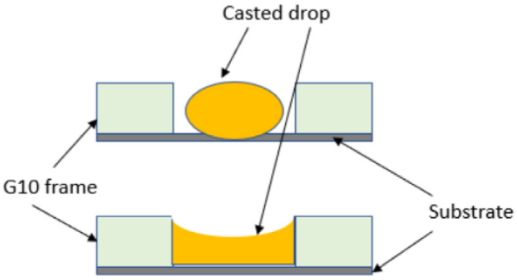

Fig. 9. Figure showing the relation of non uniformity in the target due to surface tension and size of drop.

Five different solvents or solvent mixtures were considered for making the suspension: (a) 100% distilled water, (b) 100% trichloromethane (chloroform), (c) 80% distilled water and 20% methanol, (d) 50% distilled water and 50% methanol, and (e) 50% distilled water and 50% isopropyl alcohol (IPA). The percentage values included are by volume. The deposition uniformity was found to depend on the evaporation rate. Table 1 shows the evaporation rate ER ($\mu g\, m^{-1}\, h^{-1}$) calculated using the correlation between ER as a function of vapor pressure (VP) and molar mass (M): ER =1464 * VP (Pa) * M (g/mol) given by [8].

Each homogeneous suspension was prepared by mixing 7.85 mg of HgO in 1.5 ml of solvent mentioned above. A drop of 150 μl was cast on a substrate using a micro-pipette and allowed to dry in a covered petri dish. Dried HgO target is shown Fig. 10 (a). Best results were obtained with a solvent mixture of 50%–50% distilled water and IPA. The evaporation rate for this mixture of solvents is faster than water but not as fast as methanol or chloroform. This mixture has a very low surface tension so it was necessary to make sure that any droplet does not flow out of the micro-pipette before casting on the substrate. An evaporation rate of $3.894\times10^8\ \mu g\, m^{-1}\, h^{-1}$ was achieved.

The surface tension of the solvent/solvent mixture as well as the size of the cast drop plays an important role in obtaining a uniformly thin solid target. As shown in Fig. 9, a smaller drop size will produce a convex surface whereas a larger-sized drop will fill up the cavity but give a concave surface. A multi-layer drop-casting was also attempted where a large drop was initially cast on the substrate; after the deposition dried out, another smaller drop was cast onto the existing surface. Multiple casts are performed after the previous cast dries out completely. When a cast was done over a previously existing layer, the drop should be cast gently from very low height so as not to damage the

Table 1
Solvent mixtures and their evaporation rate ER.

Solvent 1	Solvent 2	Proportion of solvents	VP at 25 °C kPa	ER(μg m^{-1} h^{-1})
Water	–	100%	3.17	8.358×10^{7}
Water	Methanol	80%–20%	4.55482	3.337×10^{8}
IPA	–	100%	4.4	3.871×10^{8}
Water	IPA	50%–50%	3.40505	3.894×10^{8}
Water	Methanol	50%–50%	7.42685	5.442×10^{8}
Methanol	–	100%	16.96	7.955×10^{8}
Chloroform	–	100%	26.6645	4.660×10^{9}

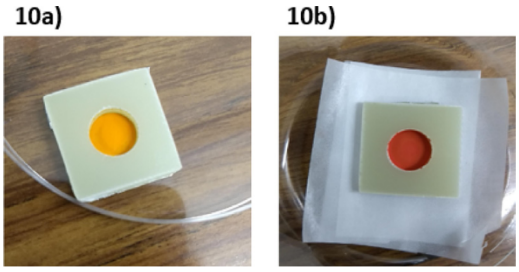

Fig. 10. Targets obtained with drop casting on Al-mylar substrate with G10 frame: (10a) drop-casting with HgO (10b) drop-casting with HgS.

structure of previous deposition. This method gives an almost uniform deposition of about 0.5% after 4 or 5 drops, with total thickness of the target ranging between 25-38 mg/cm^2 with 7 mg/cm^2 per cast. If a less concentrated solution was used, for obtaining a thin target after 4-5 drops, non-uniform deposition of higher than 0.7% was obtained because the number of particles per unit area per drop-cast decreases. Fewer particles available in each layer results in larger non uniformity.

HgS: A homogeneous suspension was prepared by mixing 0.9 ml distilled water with 0.9 ml IPA and 122.0 mg of HgS. HgS is insoluble in water as well as IPA. The vial containing the suspension was shaken at high speed using a vortex mixer for 10 min to form a colloidal suspension. A drop of 180 μl was cast into the target cavity using a micro-pipette. As HgS is insoluble in the solvent, it was necessary to shake or stir the suspension rapidly prior to filling the pipette, to ensure the collection of a homogeneously mixed suspension during casting. After casting the drop, the target was covered in a petri dish. The mixture was allowed to evaporate slowly to form a thin film (as in Fig. 10 b). Thicknesses between 7.46 mg/cm^2 and 11.04 mg/cm^2 were reproducibly obtained with this method. The weight of the substrate was measured before casting and after drying of drop, to compare the difference. Also the energy loss of ^{241}Am (5.486 MeV) through the HgS target was used to estimate the thickness. Uniform targets were obtained with non-uniformity of 0.32%.

3. Target self calibration

The HgS target was used for obtaining the nuclear reaction cross-sections of the (p, γ), (p, n) and (p, α) reaction on ^{196}Hg through the method of activation. The daughter nuclei produced in the activation initially decay though electron capture processes followed by the emission of decay photons. The reaction cross-sections are thus determined by measuring the number of emitted photons using HPGe (Hyper Pure Germanium) detectors. The background subtracted, energy calibrated proton activation spectrum of HgS obtained at 4 MeV is shown in Fig. 11. Fig. 12 shows a snippet from proton activation spectrum of HgS at irradiation energy of 6.93 MeV. The peaks of ^{198}Tl, ^{198m}Tl, and ^{200}Tl are shown.

One particularly useful feature of a HgS target is the fact that its thickness can be determined in a proton activation experiment because the cross section of ^{34}S(p,n)^{34}Cl is known. It is important to know how many ^{196}Hg nuclei are present within the incident beam area to obtain the required reaction cross-section. As the target is made up of HgS, there is one mercury atom for each sulfur atom present in the target; areal number density of sulfur nuclei n_S within the beam is equal to areal number density of mercury nuclei n_{Hg}.

Considering the contribution of secondary gamma radiation coming from daughter nuclei produced from stable sulfur isotopes, only the contribution from ^{34}Cl is important as all the other daughter nuclei are very short lived. ^{34}Cl can be produced by the (p, γ) reaction on ^{33}S and by the (p, n) reaction on ^{34}S.

The reaction cross-section of ^{34}S(p, n)^{34}Cl is experimentally measured [9]. Further, experimental measurements of the (p, γ) reaction rate indicate that this reaction is negligible compared to that of the (p, n) reaction [10] by several orders of magnitude and are well below other uncertainties in Hg activation measurements. These values also closely match Hauser–Feshbach computations [11].

Target thickness calibration can proceed in the following manner. The number of photons from a distinct ^{34}Cl peak is given by$N_{\gamma Cl34}$:

$$N_{\gamma \mathrm{Cl}34} = \sigma_{\mathrm{Cl}}\, I_{\mathrm{Cl}}\, \epsilon_{\mathrm{Cl}}\, f(t)_{\mathrm{Cl}}\, n_{\mathrm{S}34} \tag{3}$$

where $N_{\gamma Cl34}$ is number of gamma detected from any distinct ^{34}Cl peak, σ_{Cl} is the cross-section, I_{Cl} is the gamma branching ratio for an electron capture decay, ϵ_{Cl} is the absolute detector efficiency (both geometric and intrinsic) at that particular detected gamma energy, n_{S34} is areal number density of ^{34}S nuclei and $f(t)_{Cl}$ is given by:

$$f(t)_{\mathrm{Cl}} = \frac{e^{-\lambda t_t}\,(1 - e^{-\lambda t_d})}{\lambda} \cdot N_l \tag{4}$$

where t_t is duration of time taken to transfer the irradiated target to detector, t_d is the duration of detection, λ is the decay constant of daughter nuclei and N_l is given by:

$$N_l = \sum_{i=1}^{n} I_{Bi}\,(1 - e^{-\lambda \triangle t_i})\, e^{-\lambda t_{di}} \tag{5}$$

where the irradiation time is divided into small time segments of length $\triangle$t which is small compared to the timescale of variations in the average beam intensity, $\triangle t_i$ is the duration of ith time segment, t_{di} is the time elapsed from the end of the ith interval to the end of the irradiation period and I_{Bi} is incident beam intensity during the ith period [12] measured with a logging current meter connected to the beam-line Faraday cup.

The number of ^{34}S nuclei present per cm^2 within the area of beam, is then:

$$n_{S34} = \frac{N_{\gamma \mathrm{Cl}34}}{\sigma_{\mathrm{Cl}}\, I_{\mathrm{Cl}}\, \epsilon_{\mathrm{Cl}}\, f(t)_{\mathrm{Cl}}} \tag{6}$$

The abundance of ^{34}S is 4.25%. By evaluating the total number of ^{34}S isotopes per unit area in the target, we can determine the total number of S atoms, which is equal to the total number of Hg atoms per unit area.

4. Conclusion

Fabrication of a solid mercury target of ~10 mg/cm^2 can be successfully obtained using drop-casting methods described in this paper. The use of HgS for activation with an incident proton beam makes the target self-calibrating as the experimental cross-section for ^{34}S(p, n)^{34}Cl is known [9] and contributions from ^{33}S(p, γ)^{34}Cl are negligible.

Of particular astrophysical interest is ^{196}Hg. As its abundance is 0.15%, using isotopically enriched mercury compounds for making the target will result in very expensive target specimen. Using natural mercury compounds helps for producing cost-effective targets and use of techniques discussed here helps in synthesizing the required targets at standard ambient temperature and pressure. Using the described method as a proof of principle, isotopically enriched targets will be explored in future work.

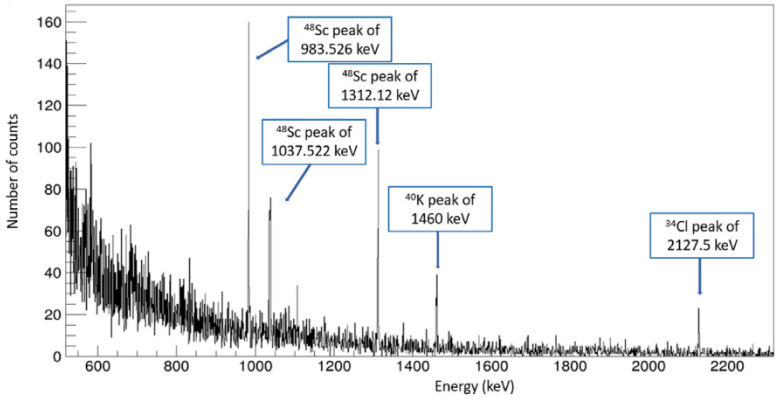

Fig. 11. Background subtracted, energy calibrated proton activation spectrum of HgS at 4 MeV. Figure shows few ^{48}Sc peaks, ^{40}K peak and ^{34m}Cl peak.

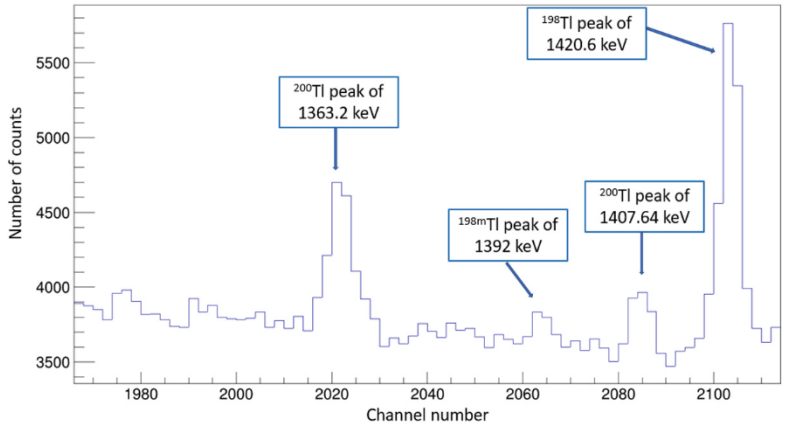

Fig. 12. Proton activation spectrum of HgS at 6.93 MeV. The peaks seen are of ^{200}Tl, ^{198}Tl, and ^{198m}Tl.

Declaration of competing interest

The authors declare that they have no known competing financial interests or personal relationships that could have appeared to influence the work reported in this paper.

Acknowledgments

This work is supported in part by National Science Foundation [grants numbers PHY-1712832, PHY-2110218].

References

[1] A. Stolarz, Target preparation for research with charged projectiles, J. Radioanal. Nucl. Chem. 299 (2) (2014) 913–931.
[2] E. Cruceanu, N. Nistor, Crystal growth of HgS from Hg-rich solutions, J. Cryst. Growth 5 (3) (1969) 206.
[3] J. Szerypo, H. Friebel, D. Frischke, R. Grossmann, H. Maier, Preparation of isotopically enriched mercury sulphide targets, Nucl. Instrum. Methods Phys. Res. A 590 (1–3) (2008) 73–75.
[4] Y.E. Titarenko, O.V. Shvedov, V.F. Batyaev, V.M. Zhivun, E.I. Karpikhin, R.D. Mulambetov, D.V. Fischenko, S.V. Kvasova, S.G. Mashnik, R.E. Prael, et al., Study of residual product nuclide yields from 0.1, 0.2, 0.8, and 2.6 GeV proton-irradiated nat-Hg targets, 2000, ArXiv Preprint Nucl-Ex/0008012.
[5] M. Perakh, H. Ginsburg, Deposition of thin films of HgS from colloidal solutions, Thin Solid Films 52 (2) (1978) 195–202.
[6] T.T.K. Nguyen, H.T. Luu, L.D. Vu, T.T. Ta, G.T.H. Le, Determination of total mercury in solid samples by anodic stripping voltammetry, J. Chem. 2021 (2021).
[7] H. W., H. F., J. Inorganic General Chem. 177 (1928) 363–380.
[8] D. Mackay, I. van Wesenbeeck, Correlation of chemical evaporation rate with vapor pressure, Environ. Sci. Technol. 48 (17) (2014) 10259–10263.
[9] C. Umbarger, K. Kemper, J. Nelson, H. Plendl, Excitation functions for the reactions S 34 (p, n) Cl 34 and P 31 (α, n) Cl 34, Phys. Rev. C 2 (4) (1970) 1378.
[10] A. Parikh, T. Faestermann, R. Hertenberger, R. Krücken, D. Schafstadler, H.-F. Wirth, T. Behrens, V. Bildstein, S. Bishop, K. Eppinger, et al., New Cl 34 proton-threshold states and the thermonuclear S 33 (p, γ) Cl 34 rate in ONe novae, Phys. Rev. C 80 (1) (2009) 015802.
[11] A. Data, N.D.T. Vols, Categories used in subject index, At. Data Nucl. Data Tables 79 (2) (2001) 335–359.
[12] M.A. Famiano, R.S. Kodikara, B.M. Giacherio, V.G. Subramanian, A. Kayani, Measurement of the (p, γ) cross sections of 46ti, 64Zn, 114Sn, and 116sn at astrophysically relevant energies, Nuclear Phys. A 802 (1–4) (2008) 26–44.